BBA - Bioenergetics 1865 (2024) 149033

Contents lists available at ScienceDirect

BBA - Bioenergetics

journal homepage: www.elsevier.com/locate/bbabio

Mitochondrial quinone redox states as a marker of mitochondrial metabolism

M. Martins Pinto [a,b,c], S. Ransac [a,c], J.P. Mazat [a,c], L. Schwartz [d], M. Rigoulet [a,c], S. Arbault [b], P. Paumard [a,c,*], A. Devin [a,c,*]

[a] CNRS, Institut de Biochimie et Génétique Cellulaires, UMR 5095, F-33000 Bordeaux, France
[b] Université de Bordeaux, CNRS, Bordeaux INP, CBMN, UMR 5248, F-33600 Pessac, France
[c] Université de Bordeaux, CNRS, IBGC, UMR 5095, F-33000 Bordeaux, France
[d] Assistance Publique des Hôpitaux de Paris, France

ARTICLE INFO

Keywords:
Mitochondria respiratory chain
Bioenergetics
Quinones
Redox state

ABSTRACT

Mitochondrial and thus cellular energetics are highly regulated both thermodynamically and kinetically. Cellular energetics is of prime importance in the regulation of cellular functions since it provides ATP for their accomplishment. However, cellular energetics is not only about ATP production but also about the ability to re-oxidize reduced coenzymes at a proper rate, such that the cellular redox potential remains at a level compatible with enzymatic reactions. However, this parameter is not only difficult to assess due to its dual compartmentation (mitochondrial and cytosolic) but also because it is well known that most NADH in the cells is bound to the enzymes. In this paper, we investigated the potential relevance of mitochondrial quinones redox state as a marker of mitochondrial metabolism and more particularly mitochondrial redox state. We were able to show that Q_2 is an appropriate redox mediator to assess the mitochondrial quinone redox states. On isolated mitochondria, the mitochondrial quinone redox states depend on the mitochondrial substrate and the mitochondrial energetic state (phosphorylating or not phosphorylating). Last but not least, we show that the quinones redox state response allows to better understand the Krebs cycle functioning and respiratory substrates oxidation. Taken together, our results suggest that the quinones redox state is an excellent marker of mitochondrial metabolism.

1. Introduction

Mitochondria are double-membraned organelles involved in major metabolic pathways essential for cellular life in eukaryotic cells. They are the site of biochemical reactions such as β-oxidation of fatty acids, Krebs cycle, oxidative phosphorylation (OXPHOS), nucleotides and amino acids synthesis, heme biosynthesis and redox signaling by reactive oxygen species (ROS) [1]. These organelles are particularly well-known for their role in bioenergetics where they convert the majority of cellular energy into ATP through both the Krebs cycle and the OXPHOS system. The Krebs cycle also produces reducing equivalents, namely NADH and $FADH_2$ (through succinate dehydrogenase), that are oxidized by the respiratory chain in the inner mitochondrial membrane. Electrons from their oxidation are transferred within the enzymatic complexes composing the respiratory chain to the final electron acceptor, oxygen. The energy provided by this electron transfer is used for the extrusion of protons from the matrix to the intermembrane space. The proton electrochemical gradient generated is used by the ATP synthase to synthesize ATP [2].

Mitochondrial and thus cellular energetics are highly constrained both thermodynamically and kinetically. The three main thermodynamical forces involved are the phosphate potential (ΔGp), the redox potential (ΔG_{NADH}) and the protonmotive force ($\Delta\mu_{H+}$). Cellular energetics is of prime importance in the regulation of cellular functions since it provides ATP for their accomplishment. However, cellular energetics is not only about ATP production but also about the ability to re-oxidize reduced coenzymes at a proper rate, such that the cellular redox potential remains at a level compatible with enzymatic reactions. In a previous paper [3], we have shown that yeast cellular proliferation rate was not controlled by ATP availability. This raised the question of a

Abbreviations: EtOH, ethanol; Q_2, coenzyme Q_2; CIII, complex III; G3P, glycerol-3-phosphate; α-KG, α-ketoglutarate; ADP, adenosine diphosphate; ATP, adenosine triphosphate; NADH, nicotinamide adenine dinucleotide; CCCP, Carbonyl cyanide 3-chlorophenylhydrazone; OAA, oxaloacetate.

* Corresponding authors at: CNRS, Institut de Biochimie et Génétique Cellulaires, UMR 5095, F-33000 Bordeaux, France.
E-mail addresses: patrick.paumard@ibgc.cnrs.fr (P. Paumard), anne.devin@ibgc.cnrs.fr (A. Devin).

https://doi.org/10.1016/j.bbabio.2024.149033
Received 29 November 2023; Received in revised form 25 January 2024; Accepted 9 February 2024
Available online 17 February 2024

possible control of cellular proliferation by the cellular redox state, namely ΔG_{NADH}. However, this parameter is not only difficult to assess due to its dual compartmentation (mitochondrial and cytosolic) but also because it is well known that most NADH in the cells is bound to the enzymes. Consequently, assessing either the total or free $NADH/NAD^+$ ratio is not fully satisfying to study the cellular redox state. The quinone redox state, which is defined as the ratio between reduced quinones and oxidized quinones, plays a central role in mitochondrial function. It mostly depends on the bioenergetics state of mitochondria (respiratory rate and protonmotive force), the OXPHOS activity and the oxygen availability.

Ubiquinones (coenzymes Q) are lipid-soluble compounds composed of a benzoquinone ring and an isoprenoid side chain [4]. The number of isoprenoid units in the apolar side chain varies depending on the species (Q_{10} in humans, Q_6 in the yeast *Saccharomyces cerevisiae*, Q_8 in *Escherichia coli*). Ubiquinones (UQ) are components of the OXPHOS system, where they function as electron carriers from all mitochondrial dehydrogenases to complex III. The benzoquinone ring can be reduced by two reversible reduction steps leading to the formation of ubiquinol (UQH2), the reduced form of ubiquinone. A partial reduction of quinones produces semi-quinone radicals ($UQ^{\bullet -}$), which are highly redox active molecules that can react with oxygen and form reactive oxygen species (ROS). Quinones have an important role in both oxidative stress and cellular redox signaling through their participation in ROS production [5].

Two methods for the measurement of the quinones redox state have been reported in the literature. The first one is the chemical extraction of quinones followed by a high-performance liquid chromatography analysis [6,7]. It allows the determination of both reduced and oxidized quinone concentrations but gives a static idea of the quinone redox state as analyses are realized at a given time. The second method is an electrochemical technique using a redox mediator to indirectly monitor the quinone redox state. As described by Moore and colleagues in the 90s [8–11] or more recently by Komlodi et al. [12], short-length chain coenzyme Q such as Q_1 or Q_2 can be used as a redox mediator to measure quinone redox state by chronoamperometry in mitochondria isolated from plant or mouse tissues. These coenzymes have a smaller isoprenoid side chain than most endogenous coenzymes Q making them more hydrophilic but still sufficiently hydrophobic to permeate mitochondrial membranes. These exogenous short-length coenzymes Q reach a thermodynamic redox equilibrium with the endogenous pool of embedded quinones before diffusing back in solution where their reduced form is oxidized by the working electrode. The redox state of the redox mediator should thus reflect the mitochondrial quinones redox state and can be followed and modulated in real time. When quinone redox states were determined with the electrochemical technique and the solvent extraction followed by HPLC analysis to determine concentrations of total reduced and oxidized quinones, similar values were obtained in membranes of different *Rhodobacter capsulatus* strains [9], in isolated mitochondria from various potato strains [10] and from soybean [13], demonstrating the reliability of the electrochemical technique. However, it is important to highlight the fact that an inactive quinones pool is detected by the extraction/HPLC method, that is not revealed by the electrochemical one [4,5]. This suggests that the quinone redox state measurement by voltammetry is not representative of the redox state of all the mitochondrial quinones but rather of a "redox active" quinone pool, which interact with the electron transport chain and is related to the respiratory activity [13,14].

In this work, we used an electrochemical method to measure the quinones redox state in mitochondria isolated from the yeast *Saccharomyces cerevisiae*, based on seminal work of Moore et al., 1988 [8]. Using coenzyme Q_2 as the redox mediator, we simultaneously measured respiratory rates and quinones redox state in a thermostatically controlled chamber specifically designed to contain the Clark electrode (O_2 consumption measurement or respiration) and the three-electrode system for the quinone redox state measurement.

We show that Q_2 is an appropriate redox mediator to assess the mitochondrial quinone redox state, which depends on the mitochondrial substrate and the mitochondrial energetic state (phosphorylating or not phosphorylating). Last but not least, we show that the quinone redox state response allows to better understand the Krebs cycle functioning and respiratory substrates oxidation. Taken together, our results suggest that the quinone redox state is an excellent marker of mitochondrial metabolism.

2. Materials and methods

2.1. Yeast strain and growth conditions

Cells from the wild-type *Saccharomyces cerevisiae* strain BY4742 (MATα; his3Δ1; leu2Δ0; lys2Δ0; ura3Δ0) were grown aerobically at 28 °C and under 180 rpm stirring in autoclaved non-fermentable lactate medium: 1 % yeast extract, 1 % bactopeptone, 0.1 % ammonium sulfate, 0.1 % phosphate and 2 % lactate, pH 5.5.

2.2. Mitochondria isolation

Yeast cells were grown on a petri dish with glycerol solid media (2 % glycerol, 1 % yeast extract, 1 % bactopeptone, pH 5.5). Yeast cell cultures were preceded by two pre-cultures (48 and 24 h before the culture). Cells were harvested in the exponential growth phase. Growth was followed at 600 nm in a spectrophotometer (Safas, France). Yeast mitochondria were isolated from protoplasts by the enzymatic method described by Guérin et al. [15]. Briefly, cells were harvested at 4 °C at 1500*g* for 10 min in a Beckman centrifuge, washed twice in cold water and resuspended in a buffer containing 0.5 M β-mercaptoethanol, 0.1 M tris pH 9.3 at 32 °C during 20 min to reduce the disulfide bridges of proteins present in the yeast cell walls. Cells were then washed twice in KCl buffer (0.5 M KCl, 10 mM, pH 7) to remove excess β-mercaptoethanol, and resuspended in a digestion buffer (1.35 M deionized sorbitol, 0.1 M EGTA, 10 mM citric acid, 30 mM phosphate, 15 mg/g of cells dry weight of zymolyase, pH 5.8) at 32 °C during 30-40 min. Protoplasts so formed were then washed twice in protoplast washing buffer (0.75 M deionized sorbitol, 0.4 deionized mannitol, 10 mM tris-maleate, 0.1 % BSA, pH 6.8) and resuspended and homogenized in a homogenization buffer (0.5 M deionized mannitol, 2 mM EGTA, 10 mM tris-maleate, 0.2 % BSA, pH 6.8) within a blender. Mitochondria were isolated by differential centrifugation in a SS34 Sorvall rotor in the mitochondrial recuperation buffer (0.8 M deionized mannitol, 0.1 M EGTA, 0.5 M Tris-Maleate, pH 6.8). Centrifugations of 8 min at 750 g were used to eliminate the cell debris. The supernatant was then centrifuged for 10 min at 12,000*g*. The pellet from the first centrifugation was passed through a Teflon Potter homogenizer to collect mitochondria that were not extracted during the first homogenization and the same series of centrifugations was repeated. The mitochondrial pellet is suspended in a minimal volume of mitochondrial recuperation buffer and homogenized again in a Teflon Potter homogenizer. Mitochondrial protein concentration was measured by the Biuret method using bovine serum albumin as a standard [16]. Mitochondrial suspension was frozen by forming beads in liquid nitrogen and stored at −80 °C. On experiment days, mitochondria were thawed by a heat-ice shock method and kept on ice.

2.3. Simultaneous measurement of O_2 consumption and quinone redox state

Oxygen consumption and quinone reduction state were measured simultaneously by chronoamperometry in a 3 ml thermostatically controlled chamber at 28 °C specifically designed to be equipped with a Clark oxygen electrode and a three-electrode system for the quinone measurement composed of a glassy carbon working electrode, an Ag/AgCl reference electrode and a platinum counter electrode. A potential of −0.8 V vs the internal Ag/AgCl reference electrode was set for the

Clark electrode (reduction potential of dioxygen into water), and a potential of +0.15 V vs the external Ag/AgCl reference was applied to the glassy carbon electrode, corresponding to the Q_2H_2 oxidation potential. Cyclic voltammetry experiments were done to control the evolution of the glassy carbon electrode responses through time. The outputs of the electrodes were connected to a potentiostat (Bio-logic SP 300) and recorded using EC-Lab software (version 1133). The working electrode was polished with 0.3 μm alumina powder diluted in water on a polishing disk by doing circles on the surface.

Mitochondria (0.2 mg/ml) were incubated in the chamber with the respiratory buffer (650 mM deionized mannitol, 0.36 mM EGTA, 10 mM tris-maleate, 5 mM KH_2PO_4, pH 6.8) after stable signals for both oxygen consumption and levels of reduced quinones were obtained. The mitochondrial suspension was constantly stirred at 750 rpm. As stated in the figures, the following effectors were injected into the chamber with Hamilton syringes: coenzyme Q_2 (4 μM), G3P (10 mM), succinate (10 mM), ethanol (10 mM), α-ketoglutarate (10 mM), pyruvate + malate (10 mM each), ADP (1 mM), antimycin A (0.5 μg/mg protein), CCCP (1 μM) and oligomycin (10 μg/mg protein). Pseudo-state 4 respiration was initiated with the addition of respiratory substrates (G3P, succinate, ethanol, α-ketoglutarate and pyruvate + malate). State 3 respiration was measured by addition of ADP, at saturating concentration (1 mM) or limiting concentrations (0.05; 0.1; 0.2 mM). Interference of the added substrates and inhibitors with the current measured by the glassy carbon electrode were tested in the absence of mitochondria. No side effects of the substrates and inhibitors used at the given concentration were observed (data not shown). Respiratory rates during different steady-states of respiration were calculated as the slope of O_2 concentration versus time (analyzed in EC-lab) and expressed as natO/min/mg protein. Steady-states of quinone redox state under both pseudo-state 4 and state 3 was evaluated as a percentage of reduced quinones relative to the current amplitude measured by the quinone electrode. Current amplitude is defined as the difference between the maximum current obtained following antimycin A addition (corresponding to the totally reduced quinone portion) and the baseline current detected in the presence of only mitochondria and Q_2 (corresponding to the fully oxidized quinone portion).

2.4. NADH measurements

NADH was measured in neutralized KOH mitochondrial extracts with NAD/NADH-Glo™ Assay from Promega.

2.5. Statistical analyses

Results are expressed as mean ± SD of Pearson, calculated in Microsoft Excel. Statistical analyses were done using GraphPad Prism software. Statistically significant differences were determined by Student's unpaired two-tailed *t*-test for two data groups comparison or by one-way ANOVA followed by a Dunnett's test for multiple means comparison to a control mean or followed by a Tukey's test for multiple means comparison. A Shapiro-Wilk normality test was performed before statistical analyses. A p-value < 0.05 was considered significant and $*p < 0.05$; $**p < 0.01$; $***p < 0.001$; $****p < 0.0001$.

3. Results and discussion

As stated above, based on a previous work by Moore et al. [8], we used an electrochemical method to measure the quinone redox state in a dynamic manner on mitochondria isolated from the yeast *Saccharomyces cerevisiae*. We used coenzyme Q_2 as a redox mediator, allowing real time determination of quinone redox state following thermodynamic redox equilibrium between the short-length quinones and the highly hydrophobic endogenous quinones pool embedded in the mitochondrial membranes (Q_6 in *S. cerevisiae*). We simultaneously measured respiratory rates and quinones redox state in a thermostatically controlled chamber specifically designed to contain the Clark electrode (O_2 consumption measurement or respiration) and the three electrodes for the quinone redox state measurement (See Materials and methods section for more details). Reduction of O_2 into water and oxidation of Q_2H_2 into Q_2 generate current variations that are proportional to each species concentration. As shown in Fig. 1, after stabilization of the signals, mitochondria were incubated in the respiratory buffer. Coenzyme Q_2 and the different effectors were then sequentially injected into the chamber.

Pseudo-state 4 was initiated by addition of a respiratory substrate (G3P) at saturating concentration and state 3 by adding saturating concentration of ADP. Reduction of O_2 into water and oxidation of Q_2H_2 into Q_2 generates an electron flow within the Clark electrode and the quinone electrode respectively, which results in currents that are proportional to the O_2 and Q_2H_2 concentrations. Respiratory rates were determined from the slope of the steady state O_2 concentration and expressed as natO/min/mg protein. We determined the quinone redox state as the percentage of quinones reduction relative to the current variation (ΔI) in each condition versus the maximum current when quinones are totally reduced (in the presence of antimycin A) and the basal current when quinones are fully oxidized (in the sole presence of mitochondria and Q_2), ΔI total. Quinone redox state was calculated as followed:

$$QH2\ (\%) = \frac{\Delta I\ (\text{pseudo} - \text{state 4 or state 3})}{\Delta I\ \text{total}} \times 100$$

3.1. Experimental validation of quinone redox state assessment

3.1.1. Determination of the optimal Q_2 concentration

Although Q_2 acts as a redox mediator to measure the quinone redox state, it could induce side effects on mitochondrial bioenergetics. At high concentration, exogenous quinones could significantly deviate electrons from the electron transport chain resulting in an increase in mitochondrial respiration or even alter the integrity of the inner mitochondrial membrane. In order to determine whether Q_2 was detrimental to

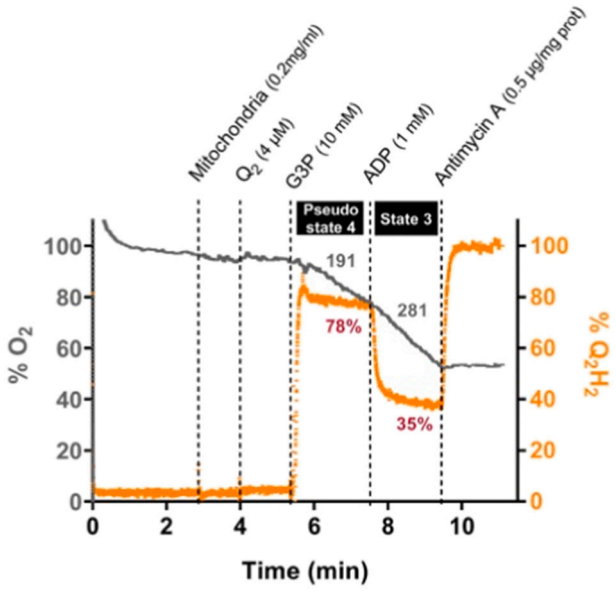

Fig. 1. Experimental determination of respiratory rates and quinone redox states. Raw data obtained for the simultaneous measurement of O_2 consumption (grey line) and the reduced quinones (orange line). Mitochondria, redox mediator Q_2, G3P, ADP and antimycin A were sequentially injected into the chamber at the concentration indicated in the figure to modulate mitochondrial respiration and quinone redox state. Pseudo-state 4 is considered to be the bioenergetics condition in which only the substrate of the respiratory chain is present and state 3 to be the phosphorylating state, when ADP is added.

mitochondrial function, we assessed respiratory rates, quinone redox state and the inner membrane electrical potential in the presence of increasing Q_2 concentrations (Fig. 2).

Mitochondrial respiratory rates with G3P as substrate were not affected up to 4 μM Q_2 in our experimental conditions. When 8 μM Q_2 was added, respiration rates were slightly increased compared to the ones in the absence of the redox mediator under both bioenergetics states (Fig. 2A). As expected, increasing Q_2 concentrations lead to a linear increase of the measured current amplitude. Indeed, since the redox mediator is not too hydrophobic, increasing the [Q_2], at a constant mitochondrial quantity, leads to an increase of the Q_2H_2 concentration in solution, which results in an increase in the measured currents proportional to the [Q_2] (Fig. 2B). Identical quinone redox states were calculated, regardless of the Q_2 concentration (Fig. 2C). Last, the redox mediator did not impact the mitochondrial membrane electrical potential upon either pseudo-state 4 or state 3 up to 8 μM (Fig. 2D). Surprisingly, while the highest 8 μM concentration did induce a slight increase in respiratory rates under pseudo-state 4 and state 3, it did not impact either the quinones redox state or the membrane potential.

Experimentally, since low current variations in the range of nanoampere (nA) were detected for the reduced quinones, increasing the Q_2 concentration increased the signal/noise ratio. We therefore decided to run our experiments with a Q_2 concentration of 4 μM, higher than the 1 μM found in the literature [8–13], but not disturbing the mitochondrial redox responses.

3.1.2. *Determination of the optimal amount of mitochondria*

We previously hypothesized that the redox mediator partitions between mitochondrial membranes and the solution. This should have an effect on free concentration of Q_2H_2 in solution and thus on the current amplitude detected by the glassy carbon electrode. We thus tested the impact of mitochondrial amount on [Q_2H_2] current amplitudes at 4 μM [Q_2]. Results are presented in Fig. 3.

Comparable respiratory rates were observed for each concentration of mitochondria, which is expected as they are normalized to the protein amounts (Fig. 3A). Increasing the concentration of mitochondria resulted in a decrease of the measured [QH_2] current amplitude (Fig. 3B) without any effect on the quinone redox state (Fig. 3C). These results are consistent with our hypothesis of an effect of the partition of Q_2 between the solution and mitochondrial membranes on the current amplitudes. Increasing the amount of mitochondria will increase membranes available for Q_2 and thus decrease its concentration in solution. We decided to work at 0.2 mg/ml of mitochondria in our experiments and keep it constant all throughout this paper.

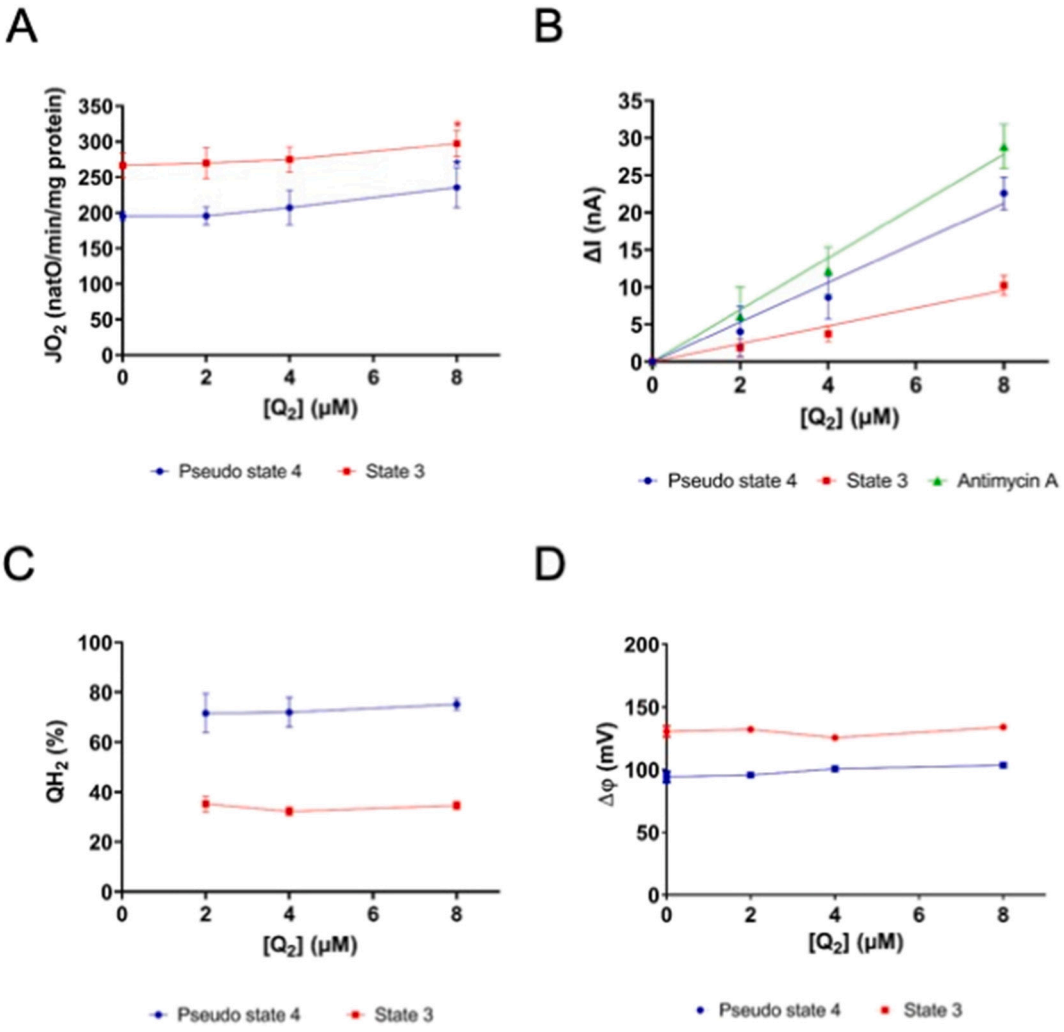

Fig. 2. Effect of exogenous Q_2 addition on (A) respiratory rates, (B) quinones current amplitude, (C) quinone redox state and (D) membrane potential. Measurements were done in the presence of 0.2 mg/ml of mitochondria, 10 mM of G3P (pseudo-state 4), 1 mM of ADP (state 3) and 0.5 μg/mg protein of Antimycin A. Results shown are means ± SD of five separate experiments done on two mitochondrial preparations for each Q_2 concentration. (A and D) Means were compared to the one without Q_2 addition by an ANOVA followed by a Dunnett's test. (B) Currents for each condition were subtracted from the baseline current measured in the presence of mitochondria and Q_2. Maximal current amplitudes are represented here.

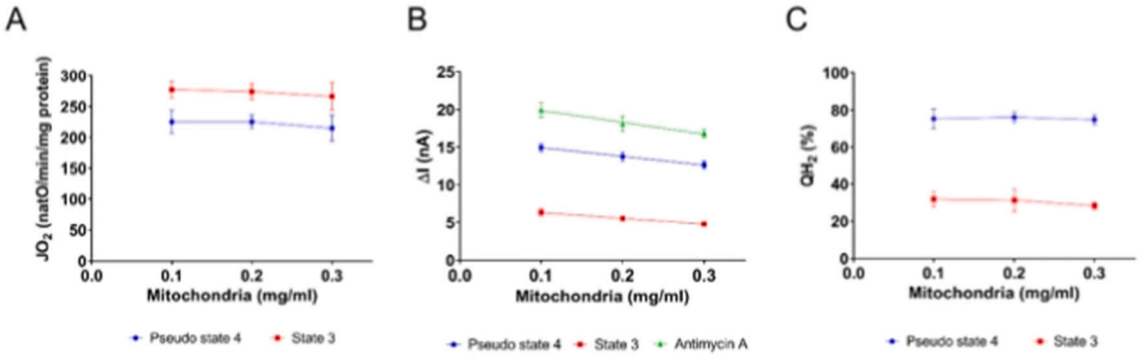

Fig. 3. Effect of the amount of mitochondria on the respiratory rates (A), the quinones current amplitude measured by the glassy carbon electrode (B) and the redox state of quinones (C). Measurements were done in presence of 4 μM of Q_2, 10 mM of G3P (pseudo-state 4), 1 mM of ADP (state 3) and 0.5 μg/mg protein of antimycin A. The amount of mitochondria in the experiments is indicated on the figure. Results shown represent means ± SD of four separate experiments done on the same mitochondrial preparation for each mitochondrial concentration.

3.1.3. *Determination of the quinone redox state*

As above-mentioned, the quinone redox state is the percentage of reduced quinones based on current variations measured versus when quinones are totally oxidized and totally reduced. Moore and colleagues defined totally oxidized quinones as the base current measured by the quinone electrode in the presence of mitochondria and Q_2 without exogenous addition of substrate, and the totally reducible quinone fraction as the amount of reduced quinones under hypoxic conditions [8–11]. Since mitochondria and Q_2 injection in the chamber have no or negligible effects on the measured currents of both the O_2 concentration and the reduced quinone portions (see Fig. 1), we defined our totally oxidized quinone level the same way. The totally reduced quinones were assessed under respiration inhibition by antimycin A. Binding of antimycin A to the Q_i site of the complex III blocks the oxidation of cytochromes b_L and b_H leading to a build-up of electrons upstream of complex III [17]. However, this inhibitor is well-known to be involved in high rates of ROS production [18] due to the semiquinones accumulation in the Q_O site. We thus wondered whether this electron leak could alter the maximal quinone redox state and compared this redox state under two conditions: in the presence of antimycin A and under hypoxia. As shown in Fig. 4, whatever the substrate, steady-state reduction levels of quinones are similar when expressed as relative to total reduced quinones in presence of the complex III inhibitor or hypoxia. From these results, it is clear that either inhibition of respiratory chain by antimycin A or hypoxic condition leads to a similar and maximal reduction of the quinone pool. We thus decided to use antimycin A to assess our totally reduced quinone fractions.

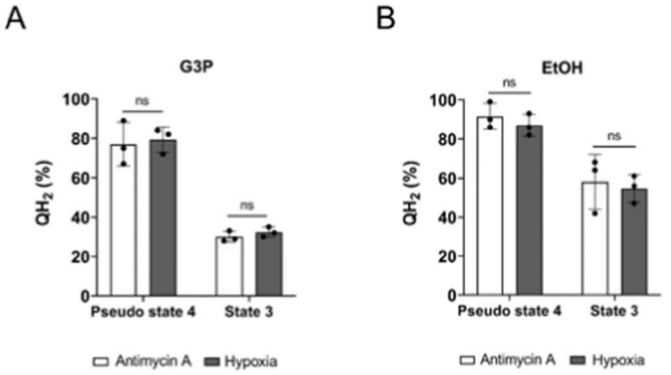

Fig. 4. Quinone reduction state when totally reduced quinones were obtained following either inhibition of mitochondrial respiration by antimycin A or hypoxia with G3P as respiratory substrate (A) or ethanol (B). Quinone redox states were assessed in presence of 0.2 mg/ml of mitochondria, 4 μM of Q_2, 10 mM of EtOH or 10 mM of G3P (pseudo-state 4) and1 mM of ADP (state 3). Either 0.5 μg/mg protein of Antimycin A or hypoxia were used to totally reduce the quinone pool. Results shown are means ± SD of three separate experiments done on the same mitochondrial preparation. Student's *t*-tests were performed to compare means of each condition under antimycin A respiration mediated inhibition or hypoxia. Respiratory rates associated with these measurements are indicated in Table 1.

3.2. *Analysis of the quinone redox state on several mitochondrial substrates*

The quinone redox state in mitochondria isolated from the yeast *Saccharomyces cerevisiae* was assessed with several mitochondrial substrates added at saturating concentrations to allow steady state establishments. Both respiratory chain dehydrogenases and Krebs cycle substrates were used (Scheme 1). It should be stressed here that NADH could not be used as a substrate since it spontaneously gives its electrons to the carbon electrode.

Three conditions were studied: substrate only (pseudo-state 4), substrate followed by addition of ADP (state 3), and substrate followed by addition of CCCP (uncoupling state). The oxygen consumption rate and quinone redox state levels were simultaneously measured under each state and are indicated in Table 1.

An increase in both the respiratory rate and the quinone redox state is observed when the substrates are added in non-phosphorylating state (pseudo-state 4), compared to the basal conditions. Substrate addition on isolated mitochondria led to an increase in the electron flow within the respiratory chain, resulting in an increase in oxygen reduction by complex IV. Both ethanol and succinate impose a high quinone redox state, with nearly all the quinones reduced whereas α-ketoglutarate only reduces 23 % of the mitochondrial quinones. In the presence of pyruvate and malate or G3P 75 % of quinones were reduced (Table 1). As shown in Scheme 1, electrons coming from the oxidation of these substrates enter the respiratory chain via different entry points. Further, reduced quinone levels following substrate addition depend on various kinetic and thermodynamic controls: the substrates transport within mitochondria, the dehydrogenase activities, the proton-motive force and CIII+CIV activity. Some of them are discussed below.

Ethanol diffuses through membranes and reduces 87 % of quinones. This respiratory substrate is converted into acetaldehyde by the matrix alcohol dehydrogenase (ADH), itself converted into acetate by the matrix acetaldehyde dehydrogenase with the generation of NADH that is then oxidized by the internal NADH dehydrogenase, Ndi (Scheme 1). After diffusion of G3P into the intermembrane space and import of succinate into the matrix through its transporter, the dicarboxylate carrier (Dic1) [19], G3P and succinate directly give their electrons to the electron transport chain (ETC) via Gut2 (the yeast glycerol-3-phosphate dehydrogenase) and the succinate dehydrogenase (complex II of the

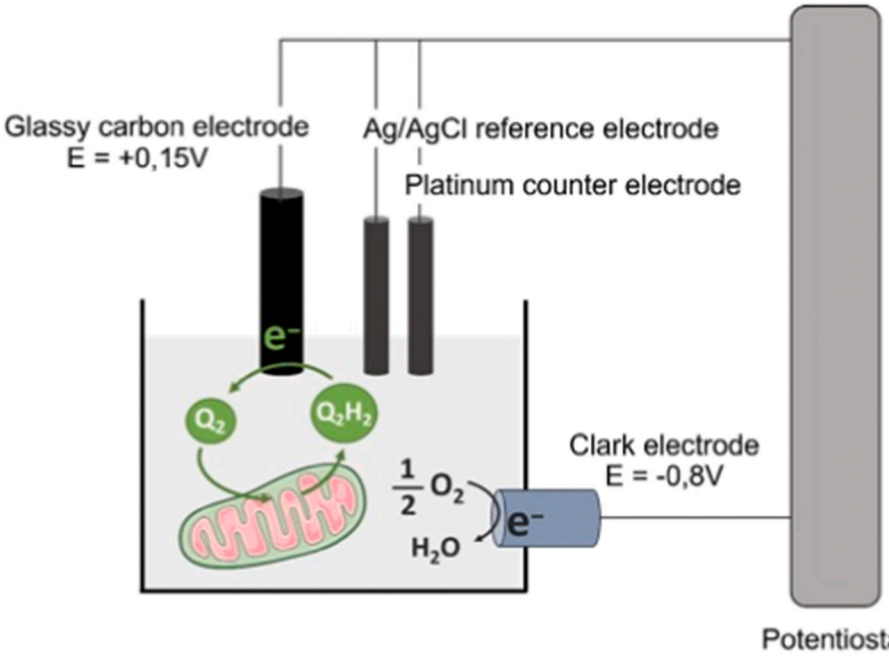

Scheme 1. Simplified scheme of the electrode-based electrochemical technique used to simultaneously monitor the mitochondrial respiration and redox state of quinones on isolated mitochondrial from yeast. A specific chamber has been designed to be equipped with a Clark electrode to measure oxygen consumption and a three-electrode system for the indirect measurement of reduced quinone levels using coenzyme Q_2 as a redox mediator. This three-electrode system is composed of a glassy carbon working electrode set at a fixed potential relative to a silver/silver chloride (Ag/AgCl) reference electrode (E = +0.15 V) and a platinum counter electrode to complete the electronic circuit.

Table 1
Respiratory rates and quinone redox state measured in isolated mitochondria from *Saccharomyces cerevisiae*. Respiratory rates and percentage of reduced quinones were simultaneously assessed in presence of 0.2 mg/ml of mitochondria, 4 μM of Q_2, 10 mM of the respiratory substrate specified in the table (pseudo-state 4), 1 mM of ADP (state 3). Uncoupling state was assessed after addition of 1 μM of CCCP in the presence of substrate only. Antimycin A (0.5 μg/mg protein) was used to totally reduce quinones. Results shown are means ± SD of at least six separate experiments done on at least six mitochondrial preparations.

Respiratory substrate	JO2 (nAtO/min/mg protein)			
	Pseudo State 4	State 3	Uncoupling state	RCR
EtOH	219 ± 29	342 ± 56	398 ± 23	1.6 ± 0.2
G3P	194 ± 27	262 ± 28	300 ± 13	1.4 ± 0.2
Succinate	214 ± 33	273 ± 37	69 ± 22	1.3 ± 0.7
α-KG	101 ± 25	266 ± 44	43 ± 3	2.9 ± 0.6
Pyruvate/malate	190 ± 20	255 ± 24	142 ± 19	1.3 ± 0.1

Respiratory substrate	QH2 (%)		
	Pseudo State 4	State 3	Uncoupling state
EtOH	87 ± 10	57 ± 11	50 ± 9
G3P	75 ± 5	30 ± 4	25 ± 4
Succinate	101 ± 7	39 ± 10	3 ± 0.7
α-KG	23 ± 6	42 ± 7	3 ± 0.5
Pyruvate/malate	75 ± 10	33 ± 7	10 ± 4

respiratory chain), respectively. The quinone redox state values obtained with these substrates indicate that succinate imposes the highest quinone redox state. When the Krebs cycle substrate α-ketoglutarate is added to isolated mitochondria and imported within the matrix by the Odc1 transporter [20], it is converted into succinyl-CoA via the α-ketoglutarate dehydrogenase (αKG-DH), resulting in the production of NADH that is then oxidized by Ndi (Scheme 1). While the electrons coming from either ethanol and α-ketoglutarate enter the ETC via Ndi, the quinone redox state values are very different. Because these substrates are not directly oxidized at the level of the ETC, NADH generated by their conversion is dependent on their transport in the mitochondrial matrix and the ADH and αKG-DH activities. α-ketoglutarate is imported into the matrix by the Odc1 carrier present in the inner mitochondrial membrane and its transport can be limited, whereas ethanol is a small molecule that can passively diffuse through mitochondrial membranes. Moreover, the activity of αKG-DH is also modulated by the Krebs cycle. Indeed, a Krebs cycle intermediate accumulation in the steps occurring after this reaction leads to a feedback inhibition of the αKG-DH resulting in a decreased activity. Pyruvate and malate are also Krebs cycle substrates transported into the mitochondrial matrix by the mitochondrial pyruvate carrier (MPC) [21] and the Dic1 transporter respectively [19]. Pyruvate is converted into acetyl-CoA by the pyruvate dehydrogenase and malate is oxidized into oxaloacetate by the malate dehydrogenase. Oxaloacetate and acetyl-CoA can then form citrate in the reaction catalyzed by the citrate synthase and the Krebs cycle can hypothetically fully function. 75 % of the total quinones are reduced when electrons come from the oxidation of these substrates.

In the presence of ADP (state 3), respiration is stimulated for all the substrates mentioned above and the quinone redox state decreases with all substrates but αKG (Table 1). As the constraint on the respiratory chain (high transmembrane electrochemical potential) is removed under phosphorylating state due to the ATP synthase activity (transmembrane proton gradient consumption), respiration rate increases to maintain the transmembrane electrochemical potential and mitochondrial quinones are oxidized as the electron flux within the ETC increases. This is in agreement with the coupling via the protonmotive force between the electron transfer within the respiratory chain and phosphorylation by ATP synthase described by Mitchell [2]. Interestingly, the

quinone redox state in the phosphorylating state with α-ketoglutarate is about two times higher than the pseudo-state 4 one. As this substrate induces the highest respiration stimulation in state 3, a significant decrease of the reduced quinones level would be expected. The observed increase indicates that there is no simple relationship between the respiratory rate and the quinone redox state.

It has been previously demonstrated in our laboratory that substrate-level phosphorylation within the Krebs cycle results in a respiratory rate increase (in the presence of oligomycin) with α-ketoglutarate as a substrate [22]. Indeed, the succinyl-CoA synthetase that catalyzes the oxidation of succinyl-CoA to succinate, requires ADP as a substrate (see Scheme 1). We hypothesized that the increase in the quinone redox state observed in presence of α-ketoglutarate and ADP was due to a stimulation of the succinyl-CoA synthetase activity, resulting in an increase of NADH production and an increase in redox pressure at the entrance of the respiratory chain. The modulation of the quinone redox state by substrate level phosphorylation with Krebs cycle substrates was further investigated below.

Maximal respiratory rates were assessed in the presence of CCCP after pseudo-state 4 induction. The uncoupler induced a slight increase in respiration and a slight decrease in the quinones redox state with G3P and ethanol as respiratory substrates whereas it inhibited respiration

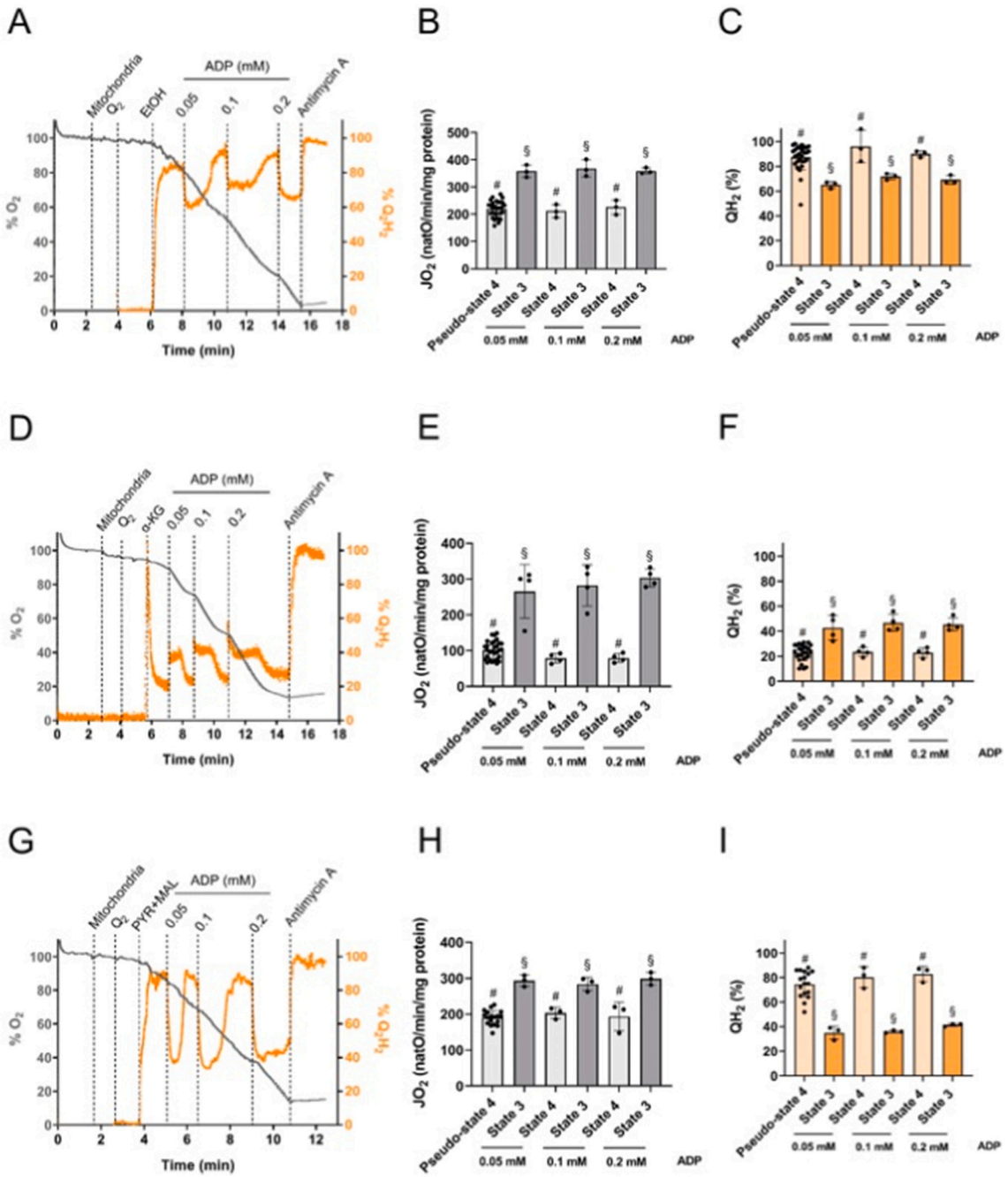

Fig. 5. Effect of limiting concentrations of ADP on the quinone redox state. Respiratory rates and percentage of reduced quinones with EtOH (A–C), α-ketoglutarate (D–F) and pyruvate + malate (G–I) as respiratory substrates were assessed in presence of 0.2 mg/ml of mitochondria, 4 μM of O_2, 10 mM of substrate, different concentrations of ADP as indicated in the figures, 1 μM of CCCP and 0.5 μg/mg protein of antimycin A. Results shown represent means ± SD of at least three separate experiments done on two mitochondrial preparations. # and § represent non-significant statistical differences between groups means indicated with the symbol according to an ANOVA followed by a Tukey's test.

and leads to a percentage of <10 % of reduced quinones with the other substrates (Table 1). Succinate and pyruvate are known to be transported within mitochondria by the dicarboxylate carrier (Dic1p) and with a proton by the mitochondrial pyruvate carrier (MPC) [21], respectively. As CCCP disrupts the proton gradient across the inner mitochondrial membrane, transport of these substrates become the limiting step, resulting in a decrease of the respiration due to a decrease in these substrates availability. Respiration was also inhibited with α-ketoglutarate, as previously described [22,23]. It has been proposed that this inhibitory effect of CCCP with α-ketoglutarate could be a consequence of a kinetic limitation by either the substrate or inorganic phosphate supplies. Indeed, it has been shown that inorganic phosphate addition restores α-ketoglutarate respiration, suggesting an impairment in the succinyl-CoA conversion into succinate coupled to ADP phosphorylation under these conditions due to the limitation of inorganic phosphate entry within the matrix, which is co-transported with a proton [23]. On the contrary, G3P passive diffusion through porin into the intermembrane space and ethanol passive diffusion within

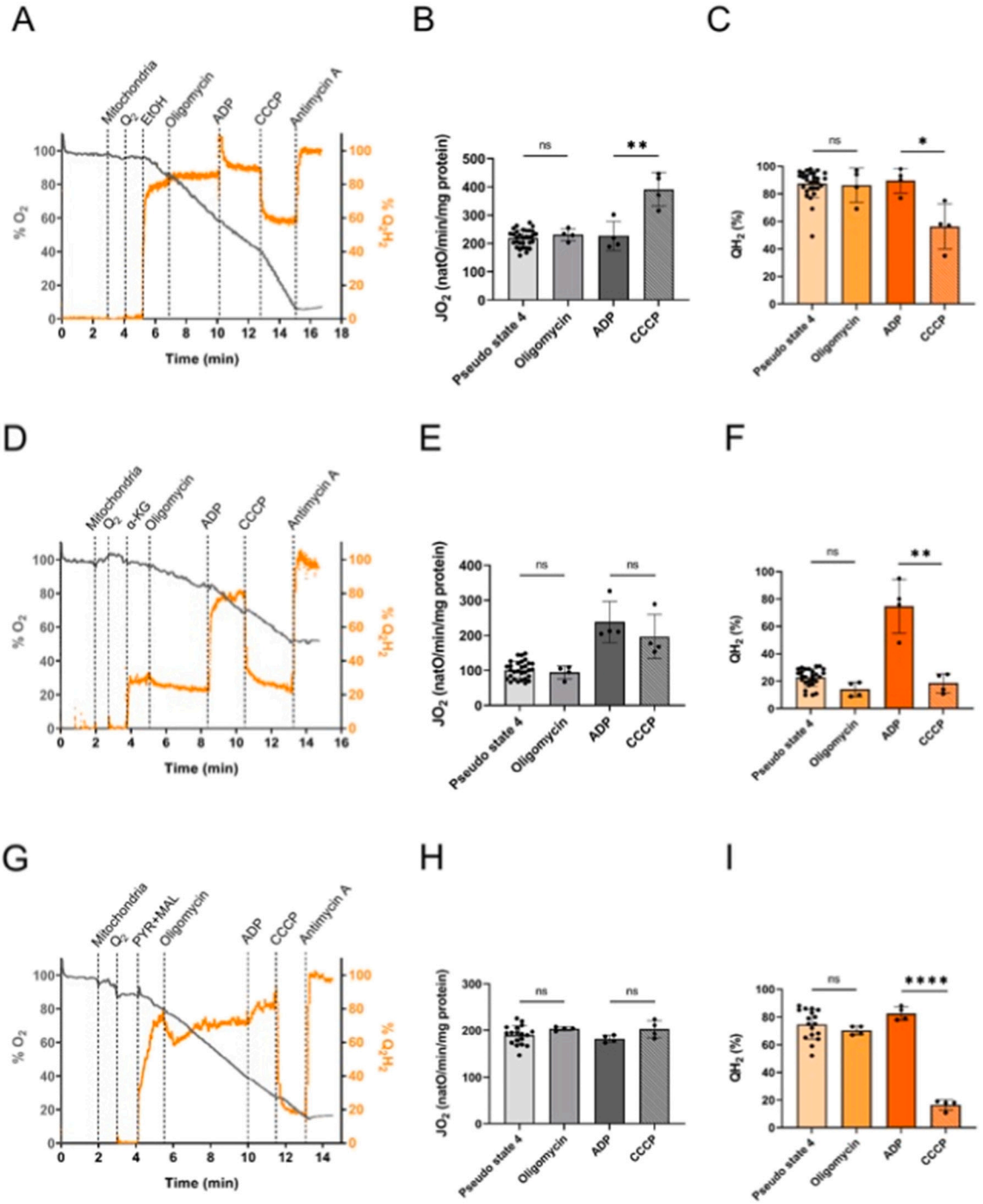

Fig. 6. Effect of ADP addition on quinone redox state when ATP synthase is inhibited. Raw data obtained of O_2 consumption and levels of reduced quinones, respiratory rates and percentage of reduced quinones with EtOH (A–C), α-ketoglutarate (D–F) and pyruvate + malate (G–I) as respiratory substrates were assessed in presence of 0.2 mg/ml of mitochondria, 4 μM of Q_2, 10 mM of substrate, 10 μg/mg protein of oligomycin, 1 mM of ADP and 0.5 μg/mg protein of antimycin A. Results shown represent means ± SD of at least four separate experiments done on two mitochondrial preparations. Student's two-tailed *t*-tests were performed to compare means of indicated conditions.

mitochondrial matrix do not require the proton gradient, which allows a greater quinone redox state under uncoupling conditions.

3.2.1. Substrate dependency of quinone redox state under phosphorylating conditions

3.2.1.1. Krebs cycle activity. The modulation of the quinone redox states in the presence of non-saturating ADP concentrations was investigated in order to determine whether the state 3 quinone redox state with α-ketoglutarate was tightly related to ADP availability. Respiratory rate and quinone redox state were assessed under sequential increases of non-saturating concentrations of ADP.

With EtOH as a substrate, rates of oxygen consumption are increased upon ADP addition as the OXPHOS is fully functioning until ADP is totally consumed and state 4 is reached, where respiratory rates are similar to the ones obtained under pseudo-state 4 (Fig. 5A and B). Quinone redox state is decreased to 60–65 % when respiration is stimulated by ADP independently of the concentration of the ADP and is increased back at the same levels as the one observed in the pseudo-state 4 upon ADP exhaustion (Fig. 5A and C).

With α-ketoglutarate as substrate, addition of non-saturating ADP concentration stimulates respiration and the redox state of quinones is about doubled when compared to the one in pseudo-state 4 (Fig. 5D–F), similarly to what was observed with saturating ADP concentration (see Table 1). Comparable values of both parameters are obtained, regardless of the ADP concentration added. The effect of ADP on the duration of both oxygen consumption rates and reduced quinone levels is dependent on its concentration. With pyruvate and malate as respiratory substrates (Fig. 5G–I), results are similar to what was obtained with EtOH with however, a lower quinone redox state under both respiratory states.

These results led us to hypothesize that for α-ketoglutarate, since the substrate level phosphorylation step takes place directly after the transformation of α-ketoglutarate into succinyl-CoA, ADP addition could stimulate α-ketoglutarate dehydrogenase leading to a large increase in the quinone redox state under state 3 compared to the pseudo-state 4.

3.2.1.2. The ADP-induced quinone reduction increase in phosphorylating state is independent of the ATP synthase. To determine whether substrate level phosphorylation itself plays a role in the modulation of the quinone redox state in the phosphorylating state for α-ketoglutarate, we assessed respiratory rate and levels of reduced quinones in the presence of oligomycin. This inhibitor blocks the proton transfer at the level of the ATP synthase subunit c ring, and thus inhibits oxidative phosphorylation-related ATP synthesis.

With EtOH as a substrate, addition of ADP had no impact on the respiratory rate and the quinones reduction level after inhibition of the ATP synthase by oligomycin (Fig. 6A–C). Addition of the uncoupler CCCP stimulated respiration up to nearly 400 nAtO/min/mg of protein leading to an oxidation of quinones of nearly 50 %, as previously shown in Table 1 (Fig. 6A–C).

With α-ketoglutarate as a respiratory substrate, ADP stimulates respiration even though the ATP synthase is inhibited by oligomycin (Fig. 6D–F). Oxygen consumption rate in the presence of ADP is comparable to the state 3 one without oligomycin (see Table 1). This was previously described and demonstrated to be due to substrate-level phosphorylation in the Krebs cycle with an increase in ATP formation [22]. Interestingly, about 70 % of quinones are reduced when the ATP synthase is inhibited, against ~40 % when the ATP synthase is functioning (see Table 1), supporting our hypothesis of an effect of substrate-level phosphorylation on the quinone redox state. In this condition, the added ADP is no longer consumed by both ATP synthase and αKG-DH but by the αKG-DH only and the effect on respiratory rate and degree of reduced quinones could be a consequence of an increase in the enzyme activity and/or an effect of the inner membrane electrochemical potential difference on the α-ketoglutarate transport. A slight decrease of respiration is induced by the uncoupler CCCP with only ~20 % of reduced quinones (Fig. 6D–F).

With pyruvate and malate as respiratory substrates, the same tendencies are observed for both respiration and reduced quinone levels as the ones measured with ethanol (Fig. 6G–I). However, it is noteworthy that the maximal percentage of reduced quinones reached in the presence of ADP is about 90 %, which is higher than the 33 % observed when the ATP synthase is functioning (see Table 1). Addition of the uncoupler CCCP slightly stimulated respiration and lead to a drop in reduced quinones.

3.2.1.3. Origin of the ADP-induced quinone reduction increase in phosphorylating state. To reinforce our hypothesis of the role of substrate-level phosphorylation in the increase in state 3 quinone redox state with α-ketoglutarate, ADP/O ratio were assessed with the above-mentioned substrates. ADP/O ratio was 1.73 ± 0.19 with EtOH; 2.23 ± 0.19 with α-ketoglutarate and 1.57 ± 0.20 with pyruvate and malate. Since yeast mitochondria have only two proton pumping sites (complex III and IV), this shows that only with α-ketoglutarate as a substrate could a significant participation of ATP synthesis through the Krebs cycle be assessed. Further, if our hypothesis stands true, ADP addition with α-ketoglutarate should activate succinylcoA synthetase and alleviate kinetic control upstream this enzyme, leading to an increase in matrix NADH, itself promoting an increase in quinone redox state. We thus assessed matrix NADH with EtOH, α-ketoglutarate and pyruvate + malate. Table 2 shows that upon ADP addition, whereas an important decrease in NADH could be assessed with EtOH as substrate, no significant variation could be measured with α-ketoglutarate or pyruvate and malate. Further, NADH seems fully reduced under state 4 condition for both EtOH and pyruvate malate but less than half reduced with α-ketoglutarate, pointing to an important kinetic control of substrate availability on NADH redox state. Consequently, an increase in matrix NADH does not seem to be responsible for the increase in quinone redox state upon ADP addition with α-ketoglutarate as substrate. Catabolism of α-ketoglutarate by the Krebs cycle will generate succinate that could be oxidized by the succinate dehydrogenase. We thus wondered whether the increase in quinone redox state upon ADP addition with α-ketoglutarate could be due to the simultaneous oxidation of NADH and succinate by the mitochondrial respiratory chain. To investigate this point, we decided to inhibit succinate dehydrogenase with OAA (Table 3). OAA is a competitive inhibitor of this enzyme which means that only about 70 % of the activity of the enzyme could be inhibited with succinate as a substrate. As expected, no significant inhibition of the respiratory rate was observed with EtOH as substrate. With α-ketoglutarate as substrate, no significant decrease of the respiratory rate could be assessed under pseudo-state 4 conditions, however, under state 3, the respiratory rate was decreased by 60 % and the quinones redox state by 80 %. With pyruvate/malate as substrates, a significant decrease in both respiratory rate and quinone redox state could be assessed in the presence of OAA indicating that with both Krebs cycle substrates, succinate generated by the Krebs cycle is reoxidized by the succinate-dehydrogenase and significantly participates in both the respiratory rate and the quinone

Table 2
NADH (% pseudo-state 4) measured in isolated mitochondria from *Saccharomyces cerevisiae*. NADH was assessed in presence of 0.3 mg/ml of mitochondria, 4 μM of Q_2, 10 mM of the respiratory substrate specified in the table (pseudo-state 4), 1 mM of ADP (state 3) and antimycin A (0.5 μg/mg protein). Results shown are means ± SD of at least six separate experiments done on two mitochondrial preparations.

NADH	Pseudo State 4 (%)	State 3 (% of Pseudo State 4)	Antimycin (% of Pseudo State 4)
EtOH	100	27 ± 7	111 ± 15
α-KG	100	109 ± 10	251 ± 42
Pyruvate/ malate	100	86 ± 13	102 ± 36

Table 3
Respiratory rates and quinone redox state measured in isolated mitochondria from *Saccharomyces cerevisiae*. Respiratory rates and percentage of reduced quinones were simultaneously assessed in presence of 0.2 mg/ml of mitochondria, 4 μM of Q_2, 10 mM of the respiratory substrate specified in the table (pseudo-state 4), 1 mM of ADP (state 3) in the presence or absence of 10 mM OAA. Antimycin A (0.5 μg/mg protein) was used to totally reduce quinones. Results shown are means ± SD of at least three separate experiments done on two mitochondrial preparations. Student's two-tailed *t*-tests were performed to compare means of pseudo state 4 and state 3 conditions in absence and presence of OAA. Statistical differences are indicated with asterisks (see correspondence in Materials and methods section). When not indicated, no significant difference was found between condition without and with OAA.

Respiratory substrate	JO2 Pseudo State 4 (nAtO/min/mg prot)		QH2 Pseudo State 4 (%)		JO2 State 3 (nAtO/min/mg prot)		QH2 State 3 (%)	
	− OAA	+ OAA	− OAA	+ OAA	− OAA	+ OAA	− OAA	+ OAA
Succinate	214 ± 33	67 ± 23 ****	101 ± 7	17 ± 3 ****	273 ± 37	39 ± 13 ****	39 ± 10	2 ± 3 ***
EtOH	219 ± 29	187 ± 36	87 ± 10	86 ± 2	342 ± 56	363 ± 28	57 ± 11	50 ± 7
α-KG	101 ± 25	88 ± 19	23 ± 6	12 ± 3 ***	266 ± 44	110 ± 20 ****	42 ± 7	9 ± 1 ****
Pyruvate/malate	164 ± 26	135 ± 14 *	46 ± 16	57 ± 3	301 ± 40	180 ± 26 **	34 ± 6	26 ± 3

redox state.

3.3. Q_2H_2 redox state and mitochondrial activity

3.3.1. Relationship between respiratory rates and quinone redox state

Mitochondrial respiration relies on electron transfers between the different complexes of the respiratory chain. The quinone pool operates in the first steps of this electron transfer through the electron transport chain by transporting electrons from the Ndi1 and succinate-dehydrogenases to complex III. We thus wondered how respiration and quinone redox state were correlated. We plotted respiratory rates against the percentage of reduced quinones obtained with the different respiratory substrates under both pseudo-state 4, state 3 and uncoupled state (Fig. 7). Our results suggest two distinct linear relationships between the rate of oxygen consumptions and the degree of quinone reductions under pseudo-state 4 and state 3. In sweet potato mitochondria, a linear relationship was observed under both state 4 and 3 bioenergetics state during sequential inhibition of the succinate dehydrogenase [11]. Under uncoupled state, a very different relationship is observed where the respiratory rate can double with very little variation in the quinone redox state. Under state 4, where the protonmotive force is high and almost constant, the highest the respiratory rate the more reduced the quinones. Under state 3, the same tendency is observed but this is a condition where the proton motive force is reduced leading to a lower quinone redox state at higher flux. Under uncoupled state, only the two substrates that do not require a carrier to be oxidized by the respiratory chain are able to maintain a somewhat high quinone redox state. If one compares the slope of the relationship obtained in the different respiratory states, there is a clear increase in this slope when the protonmotive force decreases, which shows the constraint applied by this force on the quinone redox state (Schemes 2 and 3).

4. Conclusion

In this paper, we investigated the potential relevance of mitochondrial quinone redox state as a marker of mitochondrial metabolism and more particularly the mitochondrial redox state. Since assessing mitochondrial quinone redox state requires a redox mediator, namely Q_2, its influence on mitochondrial energetic metabolism was investigated and we show that up to 4 μM, Q_2 in the mitochondrial buffer does not affect mitochondrial metabolism. Further, assessing the mitochondrial quinone redox state at various mitochondrial concentrations allowed us to show that Q_2 is mostly partitioned in the mitochondrial buffer and that the membrane partition of this molecule is only about 10 % (see Fig. 3B). While investigating mitochondrial quinone redox state on various mitochondrial substrates, we showed, as expected, that for a number of substrates mitochondrial quinone redox state decreased upon ADP addition i.e. in phosphorylating conditions. However, α-ketoglutarate behaved quite differently. Indeed, under phosphorylating conditions, the mitochondrial quinone redox state increased for α-ketoglutarate. We thus further investigated this surprising result and were able to show that this is due to the succinyl-CoA synthetase being a limiting step of this substrate catabolism within the Krebs cycle and succinate being reoxidized by succinate-dehydrogenase. This is particularly interesting since it shows that respiratory rate and mitochondrial quinone redox state are complementary measurements when investigating mitochondrial metabolism. An increase in mitochondrial respiratory rate can be associated with either a decrease (EtOH) or an increase (α-ketoglutarate) in mitochondrial quinone redox state.

CRediT authorship contribution statement

M. Martins Pinto: Methodology, Formal analysis, Data curation. **S. Ransac:** Validation, Methodology, Data curation. **J.P. Mazat:**

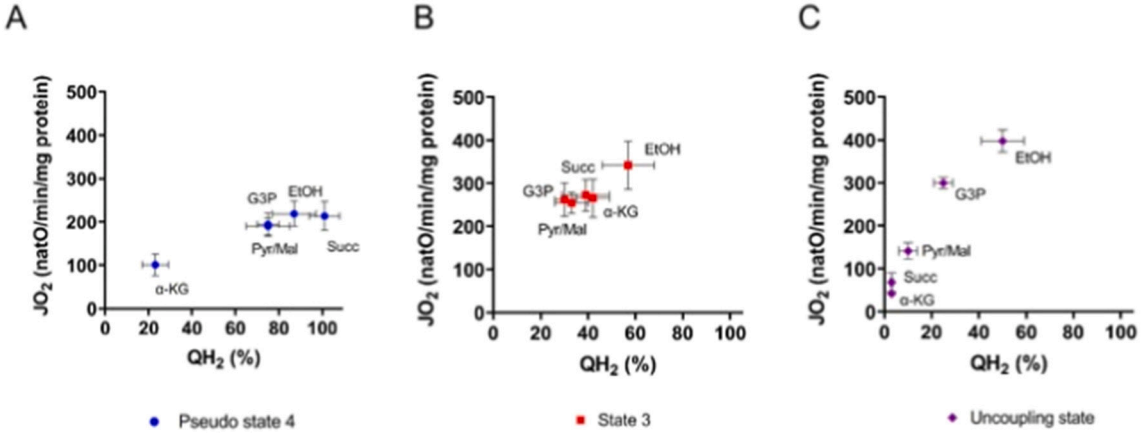

Fig. 7. Relationship between respiration and quinone redox state. Data presented in Table 1 were used to plot respiratory rates against the percentage of reduced quinones with the different studied respiratory substrates indicated in the figure, under both pseudo-state 4 and state 3.

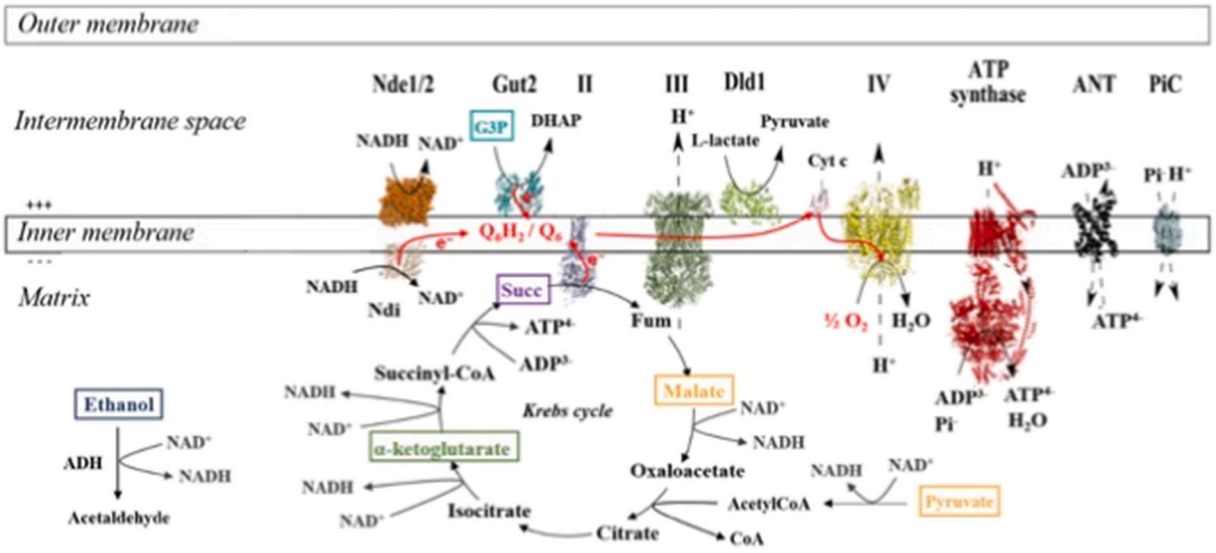

Scheme 2. Schematic representation of the OXPHOS system and the Krebs cycle in the yeast *Saccharomyces cerevisiae*. The studied substrates are framed and in colors.

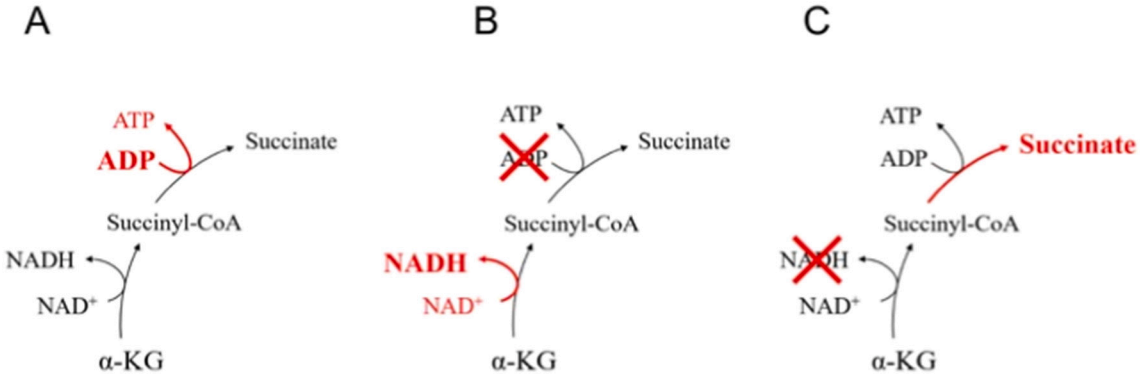

Scheme 3. Hypotheses investigated on the ADP-induced quinone reduction increase in phosphorylating state related to α-KG catabolism. Substrate-level phosphorylation was shown to be involved in the α-KG metabolization within the Krebs cycle. We first wondered whether ADP availability could be linked to the increase in quinone reduction levels at state 3 with α-KG as respiratory substrate (A; See Sections 3.1 and 3.2). It was not the case. We thus investigated if this increase in quinone redox state was promoted by a kinetic control alleviation of the succinyl-CoA synthetase by ADP addition, leading to an increase of matrix NADH production (B; see Section 3.3). It was not the case but it was due to a simultaneous oxidation by the respiratory chain of both NADH and succinate, which is also generated by the Krebs cycle (C; see Section 3.3).

Supervision. **L. Schwartz:** Supervision, Funding acquisition. **M. Rigoulet:** Validation, Supervision. **S. Arbault:** Writing – review & editing, Supervision, Methodology, Conceptualization. **P. Paumard:** Supervision, Methodology, Data curation. **A. Devin:** Writing – original draft, Validation, Supervision, Project administration, Investigation, Funding acquisition, Formal analysis, Data curation, Conceptualization.

Declaration of competing interest

The authors declare that they have no known competing financial interests or personal relationships that could have appeared to influence the work reported in this paper.

Data availability

Data will be made available on request.

Acknowledgments

This work was supported by the CNRS (Conseil National de la Recherche Scientifique), The ANR and the Fondation Guérir du Cancer, hosted by la Fondation de France. The authors are grateful to Franck Verrier for his financial support.

Appendix A. Supplementary data

Supplementary data to this article can be found online at https://doi.org/10.1016/j.bbabio.2024.149033.

References

[1] J.B. Spinelli, M.C. Haigis, The multifaceted contributions of mitochondria to cellular metabolism, Nat. Cell Biol. 20 (2018) 745–754, https://doi.org/10.1038/s41556-018-0124-1.
[2] P. Mitchell, Coupling of phosphorylation to electron and hydrogen transfer by a chemi-osmotic type of mechanism, Nature 191 (1961) 144–148, https://doi.org/10.1038/191144a0.
[3] C.L. Bouchez, N. Hammad, S. Cuvellier, S. Ransac, M. Rigoulet, A. Devin, The Warburg effect in yeast: repression of mitochondrial metabolism is not a prerequisite to promote cell proliferation, Front. Oncol. 10 (2020) 1333, https://doi.org/10.3389/fonc.2020.01333.
[4] F.L. Crane, Discovery of ubiquinone (coenzyme Q) and an overview of function, Mitochondrion 7 (2007) S2–S7, https://doi.org/10.1016/j.mito.2007.02.011.

[5] J.L. Bolton, M.A. Trush, T.M. Penning, G. Dryhurst, T.J. Monks, Role of quinones in toxicology, Chem. Res. Toxicol. 13 (2000) 135–160, https://doi.org/10.1021/tx9902082.
[6] M. Takada, S. Ikenoya, T. Yuzuriha, K. Katayama, Simultaneous determination of reduced and oxidized ubiquinones, Methods Enzymol. 105 (1984) 147–155, https://doi.org/10.1016/s0076-6879(84)05020-5.
[7] P.H. Tang, M.V. Miles, A. DeGrauw, A. Hershey, A. Pesce, HPLC analysis of reduced and oxidized coenzyme Q(10) in human plasma, Clin. Chem. 47 (2001) 256–265.
[8] A.L. Moore, I.B. Dry, J.T. Wiskich, Measurement of the redox state of the ubiquinone pool in plant mitochondria, FEBS Lett. 235 (1988) 76–80, https://doi.org/10.1016/0014-5793(88)81237-7.
[9] D. Zannoni, A.L. Moore, Measurement of the redox state of the ubiquinone pool in Rhodobacter capsulatus membrane fragments, FEBS Lett. 271 (1990) 123–127, https://doi.org/10.1016/0014-5793(90)80387-X.
[10] C.W. Van den Bergen, A.M. Wagner, K. Krab, A.L. Moore, The relationship between electron flux and the redox poise of the quinone pool in plant mitochondria. Interplay between quinol-oxidizing and quinone-reducing pathways, Eur. J. Biochem. 226 (1994) 1071–1078, https://doi.org/10.1111/j.1432-1033.1994.01071.x.
[11] I.B. Dry, A.L. Moore, D.A. Day, J.T. Wiskich, Regulation of alternative pathway activity in plant mitochondria: nonlinear relationship between electron flux and the redox poise of the quinone pool, Arch. Biochem. Biophys. 273 (1989) 148–157, https://doi.org/10.1016/0003-9861(89)90173-2.
[12] T. Komlodi, L.H.D. Cardoso, C. Doerrier, A.L. Moore, P.R. Rich, E. Gnaiger, Coupling and pathway control of coenzyme Q redox state and respiration in isolated mitochondria, Bioenergetics Commun. 2021 (2021) 3, https://doi.org/10.26124/bec:2021-0003.
[13] M. Ribascarbo, J.T. Wiskich, J.A. Berry, J.N. Siedow, Ubiquinone redox behavior in plant mitochondria during electron transport, Arch. Biochem. Biophys. 317 (1995) 156–160, https://doi.org/10.1006/abbi.1995.1148.
[14] A. Krőger, M. Klingenberg, The kinetics of the redox reactions of ubiquinone related to the electron-transport activity in the respiratory chain, Eur. J. Biochem. 34 (1973) 358–368, https://doi.org/10.1111/j.1432-1033.1973.tb02767.x.
[15] B. Guérin, P. Labbe, M. Somlo, [19] Preparation of yeast mitochondria (Saccharomyces cerevisiae) with good P/O and respiratory control ratios, in: Methods in Enzymology, Elsevier, 1979, pp. 149–159, https://doi.org/10.1016/0076-6879(79)55021-6.
[16] A.G. Gornall, C.J. Bardawill, M.M. David, Determination of serum proteins by means of the Biuret reaction, J. Biol. Chem. 177 (1949) 751–766, https://doi.org/10.1016/S0021-9258(18)57021-6.
[17] A. Osyczka, C.C. Moser, P.L. Dutton, Fixing the Q cycle, Trends Biochem. Sci. 30 (2005) 176–182, https://doi.org/10.1016/j.tibs.2005.02.001.
[18] C.L. Quinlan, A.A. Gerencser, J.R. Treberg, M.D. Brand, The mechanism of superoxide production by the antimycin-inhibited mitochondrial Q-cycle*, J. Biol. Chem. 286 (2011) 31361–31372, https://doi.org/10.1074/jbc.M111.267898.
[19] L. Palmieri, A. Vozza, A. Hönlinger, K. Dietmeier, A. Palmisano, V. Zara, F. Palmieri, The mitochondrial dicarboxylate carrier is essential for the growth of Saccharomyces cerevisiae on ethanol or acetate as the sole carbon source, Mol. Microbiol. 31 (1999) 569–577, https://doi.org/10.1046/j.1365-2958.1999.01197.x.
[20] L. Palmieri, G. Agrimi, M.J. Runswick, I.M. Fearnley, F. Palmieri, J.E. Walker, Identification in Saccharomyces cerevisiae of two isoforms of a novel mitochondrial transporter for 2-oxoadipate and 2-oxoglutarate *, J. Biol. Chem. 276 (2001) 1916–1922, https://doi.org/10.1074/jbc.M004332200.
[21] K.S. McCommis, B.N. Finck, Mitochondrial pyruvate transport: a historical perspective and future research directions, Biochem. J. 466 (2015) 443–454, https://doi.org/10.1042/BJ20141171.
[22] M. Rigoulet, J. Velours, B. Guerin, Substrate-level phosphorylation in isolated yeast mitochondria, Eur. J. Biochem. 153 (1985) 601–607, https://doi.org/10.1111/j.1432-1033.1985.tb09343.x.
[23] X. Su, M. Rak, E. Tetaud, F. Godard, E. Sardin, M. Bouhier, K. Gombeau, D. Caetano-Anollés, B. Salin, H. Chen, J.-P. di Rago, D. Tribouillard-Tanvier, Deregulating mitochondrial metabolite and ion transport has beneficial effects in yeast and human cellular models for NARP syndrome, Hum. Mol. Genet. 28 (2019) 3792–3804, https://doi.org/10.1093/hmg/ddz160.